PROCESS CONTROL OF GMAW BY DETECTION OF DISCONTINUITIES IN THE MOLTEN WELD POOL

Nancy M. Carlson, Dennis C. Kunerth, and John A. Johnson

Idaho National Engineering Laboratory
EG&G Idaho, Inc., P. O. Box 1625
Idaho Falls, ID 83415-2209

BACKGROUND

The use of ultrasonic sensors to detect discontinuities associated with the molten pool is one phase of a project to automate the welding process [1]. In this work, ultrasonic sensors were used to interrogate the region around the molten/solid interface during gas metal arc welding (GMAW). The ultrasonic echoes from the interface and the molten pool provide information about the quality of the fusion zone and the molten pool. This information can be sent to a controller that can vary the welding parameters to correct the process. Previously ultrasonic shear waves were used to determine if the geometry of the molten/solid interface was indicative of an acceptable weld [2,3]. In this work, longitudinal waves were used to interrogate the molten weld pool for discontinuities. Unacceptable welding conditions that can result in porosity, incomplete penetration, or undercut were detected.

EXPERIMENTAL PROCEDURE

GMAW was performed using a Linde side-beam welder and a Cobra-matic wire feeder. The welding parameters included currents from 212 to 310 A, voltages from 22 to 28 V, travel speeds from 0.23 to 0.27 m/min, and wire feed rates of 7.9 to 12.4 m/min using 1.1 mm feed wire. The average deposition rate was 1.4 g/s. The spray transfer mode was used with a contact-tip-to-work distance of 15.9 mm. The cover gas was 98% argon and 2% oxygen. The welds were made on 25.4 mm thick carbon steel plate with a single bevel V-groove having a 60° included angle on the bevel side, a 90° angle on the straight side, a 4.5 to 8.0 mm root opening, and a 6.4 mm backup bar.

An encoder was mounted on the side-beam welder and data were acquired during welding at 0.32 mm intervals as the electrode moved along the weld preparation. The transducer was pulsed and the echo data digitized using a CAMAC based, computer controlled workstation [4,5]. The system has the capability to move the transducer in tandem with the weld electrode. Data were also acquired with the transducer placed at a fixed, known position while the weld electrode moved past the stationary transducer.

An initial study was conducted to determine the capability of longitudinal acoustic waves to detect discontinuity conditions in the molten weld pool during GMAW. Refracted longitudinal waves were used primarily because they can propagate into the molten weld pool and allow inspection of the pool's interior during the welding process.

A single-element piezoelectric transducer, operated in the pulse-echo mode, was mounted on a lucite wedge such that 45° refracted longitudinal waves were generated in the carbon steel. The transducer, positioned 25.4 mm from the bottom corner of the weld preparation, was moved in alignment with the electrode throughout the welding pass. A-scan signals from two flaw generating conditions (porosity and incomplete sidewall penetration) and from good weld (Fig. 1) were acquired. The first A scan shows echo signals from the benign, geometric reflectors in the weld preparation prior to welding. These reflectors include the bottom corner (reflection B), the sidewall preparation (reflection C), and multiple, internal reflections from the lucite wedge (reflection A).

The second A scan in Fig. 1 shows that when the root pass penetration is adequate, no significant reflectors from the molten pool are observed. If incomplete sidewall penetration does occur on the root pass (third A scan), the bottom corner signal is still present because the corner geometry is not significantly altered by the welding process. Porosity (fourth A scan) in the molten weld pool results in a set of dynamically changing reflections that occur later in time than the original bottom corner reflection. The last three A scans in Fig. 1 can be discriminated visually, which implies that an expert system could be developed to distinguish these three welding conditions [2,6].

The results of this initial study demonstrated that refracted longitudinal waves could provide information about two unacceptable welding conditions, porosity and incomplete sidewall penetration. However, multiple reflections introduced by the transducer wedge provide no information about the welding process and complicate signal interpretation. For these reasons, a 5 MHz broadband, dual-element ultrasonic transducer that produces a 45° refracted longitudinal wave, focused at the bottom corner of the 25.4 mm thick carbon steel sample, was selected. This transducer generates the acoustic signal with one element and receives the reflected signals with the second, thereby preventing wedge multiples from interfering with the signals of interest. For this phase of the study, the transducer was fixed and not moved with the weld electrode.

Destructive examinations were made on 15 different weld root passes, along the transducer sound centerline, to determine the quality of the weld. The destructive samples show the geometry of the weld pool and the presence of incomplete penetration, acceptable penetration, undercut, and porosity.

ANALYSIS TECHNIQUES

Echoes are received from the sidewall preparation prior to the root pass. During welding these echoes are reduced in amplitude because the molten metal penetrates the sidewall. To understand the sound paths of the three reflected signals (Fig. 2) received from the sidewall preparation using the dual element transducer, a ray-tracing computer code was used. The code assumes that the sound entrance point is 25.4 mm from the edge of a 25.4 mm thick carbon steel weld sample with a 90° sidewall weld preparation. The code calculates reflection angles for

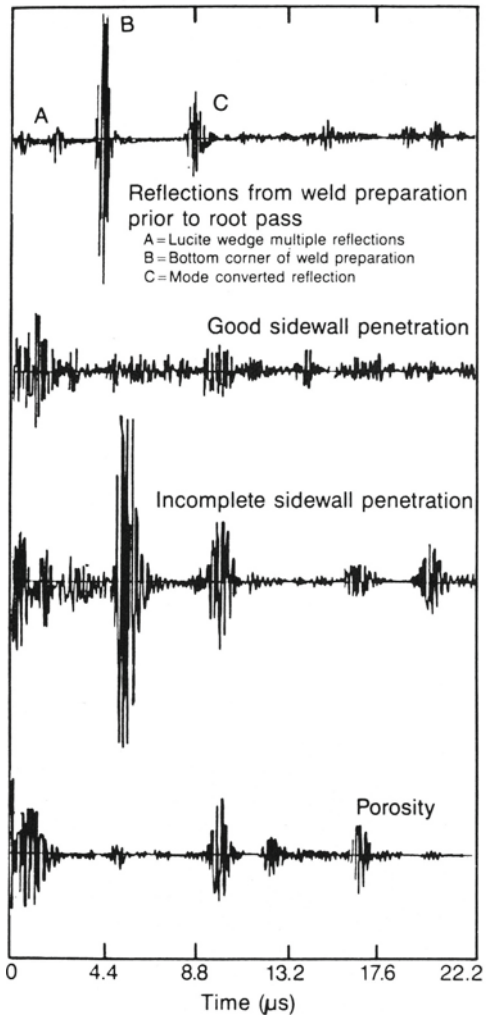

Fig. 1. A scans of weld preparation prior to and during the root pass of good and flawed weld acquired with a single element transducer.

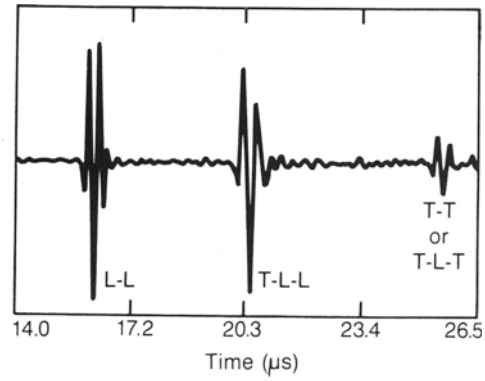

Fig. 2. A scan of weld preparation acquired with dual element transducer.

refracted, reflected, and mode-converted sound waves, provided that the outgoing ray is not beyond a critical angle. The code draws the sidewall preparation, traces rays, and outputs a graphical representation (Fig. 3). The coordinates of the ray intersection at each boundary are calculated as well as the transit time for the entire ray path.

The ray traces shown in Fig. 3 were used to analyze the three signals in the A scan of Fig. 2. The signal at 15.6 μs is generated by a refracted longitudinal wave (L-L) at 45° that is reflected at the bottom corner (Fig. 3a). The signal at 19.8 μs could result from two sound paths, each of which has three parts. The first possible sound path (Fig. 3b) consists of an initial transverse ray at 27°, which mode converts at the bottom surface to a longitudinal ray, intersects the sidewall preparation at 8.4 mm, and reflects to the top surface entering the lucite wedge at a final angle of 56°. (This path is called

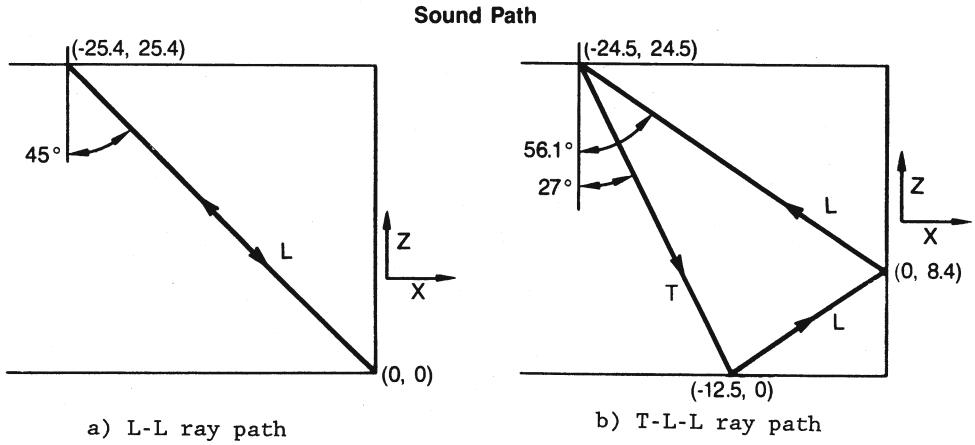

a) L-L ray path

b) T-L-L ray path

Fig. 3. Traces for rays from the transducer to the weld preparation.

T-L-L, meaning transverse-longitudinal-longitudinal.) The other path, L-L-T, is generated by an initial longitudinal leg at 33.8° that reflects off the bottom and mode converts to a transverse wave at 12.5 mm up the sidewall. This wave enters the lucite wedge at an angle of 63°. The third signal, at 25 μs, observed in a few pre-weld A scans, may be generated by either a transverse wave in the bottom corner (similar to Fig. 3a) (T-T) or by an initial transverse ray to the bottom surface at 14.8 mm that mode converts to longitudinal, intersects the weld preparation at 14.8 mm, and mode converts to transverse (T-L-T).

A second computer program [7,8] is used to determine the approximate beam spread of the sound field at the -20 dB point. From the field of the transducer, the relative amplitudes of the signals discussed above can be determined. This code calculates the magnitude of the sound field at locations along the bottom surface of the weld sample (x direction) and along the sidewall preparation (z direction) for the transducer placed on the steel sample at coordinates (x=-25.4, z=25.4). The calculated longitudinal beam spread in the x direction (bottom of sample) is 11 mm from the bottom corner. In the z direction (up the sidewall from the corner) the distance is 10 mm. These distances represent the position at which the ultrasonic intensity is down by 20 dB compared to that at the centerline of the transducer. For the refracted transverse beam, the beam spread along the bottom (x direction) is 10 to 23 mm from the bottom corner with no significant sound field on the vertical sidewall. Because of reciprocity, the effect of the beam spread on the amplitude of a received signal is expected to be the same as that on a transmitted signal to the same position.

Examining the different signals discussed above in light of the expected beam spread, some judgments about their relative amplitudes can be made. The L-L signal to the corner (Fig. 3a) is obviously along the centerline of the transducer and should be large. The L-L-T path is not expected to have a large amplitude. The initial longitudinal ray arrives at the bottom at 8.4 mm from the corner, within the 20-dB limit of the beam. However, the final transverse ray comes from a position on the sidewall, well beyond the transverse wave beam spread of the transducer. On the other hand, the T-L-L path should have a large amplitude since both the initial and final rays are within the beam spread of the transducer. Thus the second signal in Fig. 2 must be due to this combination of waves.

The T-T combination should not be too large since the corner is outside the beam spread for both the initial and final transverse legs. Finally, in the case of the T-L-T combination, the transverse ray to or from the sidewall is beyond the beam spread of the transducer and is not expected to be large. In Fig. 2 this ray is observed, but it is smaller than the other two discussed above and is not observed in other sidewall preparation A scans.

EXPERIMENTAL RESULTS

Photomicrographs and A scans for two welds are presented in Figs. 4 and 5. The three A scans below each photomicrograph are of the digitized acoustic signal obtained prior to the root pass, as the molten weld pool passed the transducer, and just after the molten weld pool solidified. These data were analyzed to determine if incomplete penetration, porosity, or undercut defect conditions could be detected by the various sound paths present in the weld sample. Penetration of the 60° bevel side of the weld preparation was not achieved in Fig. 5, and the bevel portion of the preparation is not present in the sectioned sample.

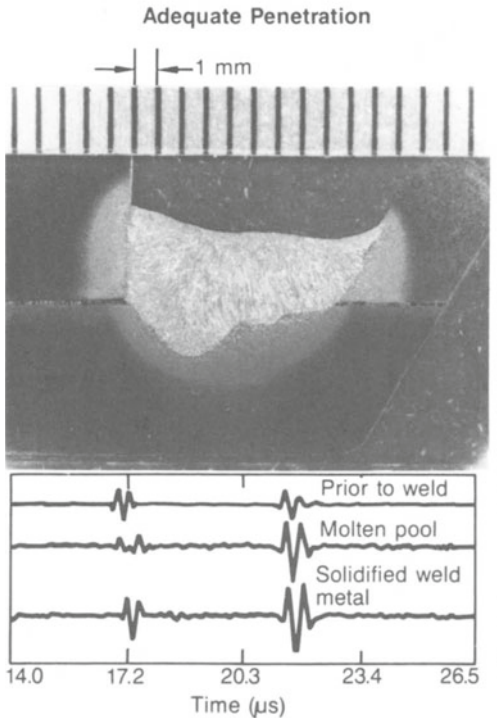

Fig. 4. Polished and etched weld sample of adequate penetration with A scans acquired using a stationary transducer prior to welding, with molten pool, and of solidified weld metal.

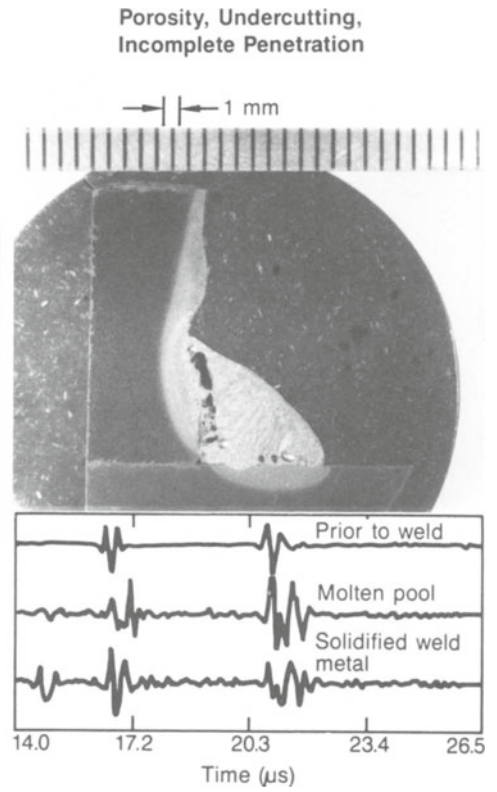

Fig. 5. Polished and etched weld sample of porosity, undercut, and incomplete penetration with A scans acquired using a stationary transducer prior to welding, with molten pool, and of solidified weld metal.

Complete penetration of the bottom corner is shown in Fig. 4, but with a low fill level of only 4 mm. The pre-weld A scan does not contain a distinct T-T signal, but the L-L and the T-L-L signals occur at 16.6 and 21.0 μs, respectively. In the presence of the molten weld pool, the L-L signal decreases significantly in amplitude and the waveform changes. The corner reflector, although reduced in amplitude, is still present because the low fill level of this root weld does not affect all of the L-L sound path. Considering that the beam spread is ~10 mm in both the x and z plane and only the main portion of the beam is not contributing to the reflected signal, 60% of the beam is sending and receiving sound energy from the corner. The T-L-L is not affected by this weld because the fill level is below 8 mm and undercut is not present to alter the sound path. In the third A scan of Fig. 4, which shows the signal received from the solidified weld, the corner signal and the T-L-L signal are observed. A low amplitude signal is also present at 18.2 μs which may be due to a specular path from the bottom surface to the solidified weld/air interface. In this case, the specular path is not at an optimum angle for reception by the receiving element, but the specular reflection is a very significant signal if the fill slope angle is between 40 and 45°.

When the welding process results in incomplete penetration, porosity, and severe undercutting, the bottom corner reflector remains when the molten pool is present, see Fig. 5. The T-L-L signal in both the molten pool and solidified A scans is reduced in amplitude and the waveform altered dramatically because of severe undercutting. The signal at 14.3 μs is most probably due to the presence of gross porosity adjacent to the sidewall. A longitudinal wave intersects the sidewall in the area of the porosity and is reflected back directly to the transducer. The porosity indication is present in both the molten and solidified A scans, but the best indication is the A scan from the solidified metal.

CONCLUSION

The analysis of welding data acquired at fifteen stationary transducer locations on a single bevel V-groove during root passes shows that certain defect conditions can be detected using refracted longitudinal sound waves. Undercut above 8 mm can be detected by the mode-converted path (T-L-L) because of the distortion effect the undercut has on the signal. This distortion can be observed as a decrease in the amplitude of the signal and a change in the waveform. Incomplete penetration can be detected at the molten pool if it occurs at the sidewall. Although the weld fill slope is a feature of the weld geometry, the fill slope can be detected if it is between 40 and 45° as the pool solidifies and, in some cases, when the molten pool is present.

An expert system could be used to determine defect conditions during GMAW by monitoring the initial weld preparation signals from a dual element ultrasonic transducer for amplitude decreases and waveform changes. The system could also monitor the molten pool A scan for additional signals that develop due to defect conditions and weld geometry. The expert system would then provide an input signal to a closed-loop process control system to minimize the amount of unacceptable root weld in an automated welding process.

ACKNOWLEDGMENTS

This work was supported by the U.S. Department of Energy, Office of Energy Research, Office of Basic Energy Sciences, under DOE Contract No. DE-AC07-76ID01570. The authors acknowledge the contribution of Gary Fletcher, who sectioned and polished the weld samples.

REFERENCES

1. J. A. Johnson et al., "Automated Welding Process Sensing and Control," Proceedings of the Second International Symposium on the Nondestructive Characterization of Materials, New York: Plenum Publishing Corp., 1986, pp. 409-417.
2. N. M. Carlson and J. A. Johnson, "Ultrasonic Sensing of Weld Pool Penetration," to be published in Welding Journal.
3. N. M. Carlson and J. A. Johnson, "Ultrasonic Detection of Weld Pool Geometry," Review of Progress in Quantitative NDE, 6B, D. O. Thompson and D.E. Chimenti, eds., New York: Plenum Publishing Corp., 1987, pp. 1723-1730.
4. J. A. Johnson et al., "Ultrasonic and Video Computerized Data Acquisition for Automated Welding," Proceedings of the 2nd International Conference on Computer Technology in Welding, The Welding Institute, 1988, pp. 18-1:18-9.
5. J. A. Johnson et al., "A CAMAC Based Ultrasonic Data Acquisition Workstation", Materials Evaluation 45, 1987, pp. 934-938.
6. J. A. Johnson, N. M. Carlson, H. B. Smartt, Gas Metal Arc Defect Formation Mechanisms: Detection and Control, EGG-SD-7405, October 1986.
7. J. A. Johnson and D. M. Tow, "Numerical Calculations of Ultrasonic Field/Crack Interactions," Review of Progress in Quantitative NDE, 5A, D. O. Thompson and D. E. Chimenti, eds., New York: Plenum Publishing Corp., 1986, pp. 83-91.
8. J. A. Johnson, N. M. Carlson, D. M. Tow, "Ray-Trace Calculations of Ultrasonic Fields," J. Acoustical Society of America 79, 1986, p. S77.